Plasma-Wall Interaction Studies in the Full-W ASDEX Upgrade during Helium Plasma Discharges

A Hakola[1]‡, S Brezinsek[2], D Douai[3], M Balden[4], V Bobkov[4], D Carralero[4], H Greuner[4], S Elgeti[4], A Kallenbach[4], K Krieger[4], G Meisl[4], M Oberkofler[4], V Rohde[4], P Schneider[4], T Schwarz-Selinger[4], A Lahtinen[5], G De Temmerman[6], R Caniello[7], F Ghezzi[7], T Wauters[8], A Garcia-Carrasco[9], P Petersson[9], I Bogdanovic Radovic[10], Z Siketic[10], ASDEX Upgrade Team, EUROfusion MST1§

[1] VTT Technical Research Centre of Finland Ltd., P.O. Box 1000, 02044 VTT, Finland

[2] Forschungszentrum Jülich GmbH, Institut für Energie- und Klimaforschung – Plasmaphysik, Partner of the Trilateral Euregio Cluster (TEC), 52425 Jülich, Germany

[3] CEA, IRFM, 13108 St. Paul Lez Durance Cedex, France

[4] Max-Planck-Institut für Plasmaphysik, Boltzmannstrasse 2, 85748 Garching, Germany

[5] University of Helsinki, Department of Physics, Association EURATOM-Tekes, P.O. Box 43, 00014 University of Helsinki, Finland

[6] ITER Organization, 13067 St. Paul Lez Durance Cedex, France

[7] Istituto di Fisica del Plasma – CNR, Via. Cozzi 53, 20125 Milan, Italy

[8] Laboratory for Plasma Physics, ERM/KMS, Partner of the Trilateral Euregio Cluster (TEC), 1000 Brussels, Belgium

[9] Department of Fusion Plasma Physics, Royal Institute of Technology, 10044 Stockholm, Sweden

[10] Rudjer Boskovic Institute, P.O. Box 180, 10002 Zagreb, Croatia

E-mail: `antti.hakola@vtt.fi`

Abstract. Plasma-wall interactions have been studied in the full-W ASDEX Upgrade during its dedicated helium campaign. Relatively clean plasmas with a He content of ¿80% could be obtained by applying ICWC discharges upon changeover from D to He. Surface analyses of W samples, however, indicated co-deposited layers with significant amounts of He and D being locally formed albeit globally D was released from the plasma-facing components. When exposing W samples to ELMy H-mode helium plasmas in the outer strike-point region of the divertor, no net erosion was observed but the surfaces had been covered with co-deposited layers mainly consisting

‡ Corresponding author

§ See the author list of "Overview of progress in European Medium Sized Tokamaks towards an integrated plasma-edge/wall solution" by H Meyer *et al*, to be published in Nuclear Fusion Special issue: Overview and Summary Reports from the 26$^{\text{th}}$ Fusion Energy Conference (Kyoto, Japan, 17-22 October 2016)

of W, B, C, and D. The layers were the thickest in the private flux region and extended throughout the OSP region in the case of rough and modified surfaces. Also, no clear signs of nanostructure growth or destruction could be seen. The growth of such layers may impact the operation of future fusion reactors. Retention of He, for its part, remained small and uniform throughout the strike-point region although our results indicate that samples with smooth surfaces contained 2-4 times less He than their rough counterparts.

1. Introduction

ITER has selected tungsten (W) to be used in the plasma-facing components (PFCs) of its divertor structures due to the good power-handling capabilities of W, low physical sputtering of W surfaces by plasma bombardment, and small retention of radioactive tritium (T) in the PFCs [1]. So far, the majority of the plasma-wall interaction studies in tokamaks with partial or full W coverage, including JET [2] and ASDEX Upgrade (AUG) [3], have been carried out in hydrogen (H) or deuterium (D) plasmas but recently also helium (He) has gained increased research interest. This is due to the possible start-up phase of ITER with helium, as well as alpha particles produced in D-T fusion reactions in its active phase, setting the need to understand in detail the interaction processes between W and He.

The most important research topics are quantifying the erosion, re-deposition, surface modification, and retention characteristics of W PFCs in different types of He plasmas. In addition, a smooth start of plasma operations in helium requires cleaning the vessel wall from residual fuel species of earlier discharges (e.g., H and D) as well as from various impurities (such as boron (B), carbon (C), nitrogen (N), and oxygen (O)) [4]. Compared to operations in H or D, during He plasma exposure nanoscale structures may develop on W-based wall components if the surface temperature, T_{S}, exceeds 1000 K (but stays well below 2000 K to prevent W from re-crystallizing and thus the PFCs from losing their hardness and strength [1]), the impact energy of He ions is $E_{\mathrm{in}} > 20$ eV, and the fluence, ϕ, is larger than $1-2\times10^{24}$ He^{+} m^{-2} [5,6]. Under such conditions, helium starts inducing bubbles in W, which will modify the surface in the nanometer scale resulting in the formation of a porous surface layer with coral-like tendrils, referred to as *fuzz*.

A critical question is if these surface modifications take place during ELMy H-mode operations of ITER and if they have a negative impact on the plasma performance or if they lead to deteriorated power-handling capabilities of the W PFCs or generation of excess dust in the vessel. Equally important is to clarify how the retention characteristics of the wall structures are altered. Interestingly, laboratory experiments indicate retention to be reduced both when exposing W samples to He-seeded H or D plasmas or when pre-treating the W surfaces with He before their exposure to H/D plasmas [7–9]. This is attributed to the above-mentioned formation of the nanoscale He bubbles which act as a diffusion barrier close to the surface, preventing hydrogen from diffusing deeper

into the bulk. However, the situation may be different in a reactor environment where thick D- or T-rich co-deposited layers can form, being the most prominent on rough and modified surfaces [10].

Fuzz generation has been experimentally observed in several linear plasma devices [5, 6, 11, 12] while identifying the onset of fuzz formation in tokamaks and temporal evolution of the modified surface layers during the plasma exposure are now a subject of joint experiments in different devices. Pioneering work has been carried out in the TEXTOR [13], Alcator C-Mod [14], and DIII-D [15] tokamaks. The TEXTOR experiments revealed that the flux of low-Z impurities (in this case C) is an additional factor determining whether the W nanostructures are grown or whether they are eroded by the impurity ions or even covered by deposits consisting of W itself and the low-Z impurities – even though all the criteria listed above were fulfilled. This was verified in C-Mod where the absence of low-Z impurities made it possible to observe nanostructure growth during a series of He discharges. The DIII-D experiments, for their part, show that transient power loads up to 0.1 MJ m^{-2} in He plasmas do not lead to damage or roughening of the exposed W surfaces. This was true for both virgin samples and for samples pre-treated in PISCES-A with a pure He beam. On the other hand, reduced gross erosion was measured for the sample having pre-formed fuzz on it while after the experiment a 30-nm deep layer consisting of nano bubbles was identified on all the samples, after only a single discharge and remaining largely unaltered with accumulating fluence.

In this contribution, we discuss the lessons learnt from two plasma-wall interaction experiments, carried out in AUG during its dedicated helium campaign in 2015. The main focus points are the efficiency of Ion Cyclotron Wall Conditioning (ICWC) in reducing the amount of deuterium in the AUG vessel upon changeover from D to He plasma operations as well as determining the erosion, deposition, fuel retention, and surface modification patterns of different W samples, some of them being pre-treated by a helium beam in the high heat-flux device GLADIS, after their exposure to ELMy H-mode discharges in He. The results have been obtained by using standard plasma discharges while the full scenario development in He took place only afterwards. Since then, advances have been made in developing ITER-relevant scenarios and efficiently controlling edge-localized modes (ELMs) using resonant magnetic perturbations under a large range of pedestal collisionalities. Interestingly, fuelling efficiency is much higher in He than in D plasmas in AUG, resulting in lower divertor pressures at comparable pedestal pressures and hotter divertor plasmas, thus influencing PWI processes.

The article is organized as follows. Section 2 discusses the ICWC method and presents the results of the cleaning experiment carried out. In section 3, erosion, deposition, and surface modifications of the W PFCs resulting from the H-mode plasma experiment are reported while section 4 concentrates on the retention of He and D on the analyzed W samples. Finally, conclusions are drawn and further steps are outlined in section 5.

2. Start-up of helium plasma operations in AUG

Depending on the plasma operations carried out in a fusion device, the first wall may need to be regularly conditioned to assist obtaining breakdown during subsequent plasma discharges or to recovering from disruptions. Wall conditioning can also assist in removing T from the reactor and cleaning the vessel walls from residual fuel inventories when switching from one plasma gas to another. Typically, conditioning is done by DC-glow discharges but they cannot be used in future reactors where the magnetic field will be continuously maintained. To this end, ICWC is a good candidate, and it has already been tested in, e.g., JET, AUG, TEXTOR, and Tore Supra [4, 16]. In ICWC, low-temperature (electron temperature $T_e < 10$ eV) and low-density (electron density $n_e = 10^{16} - 10^{18}$ m^{-3}) plasmas are formed resulting in a substantial flux of charge-exchange (CX) neutrals onto the wall structures. Such particles can mobilize the fuel and impurity atoms residing in the material, resulting in removal rates up to 10^{17} D m^{-2} s^{-1} [16].

At JET, D_2-ICWC discharges were applied after loading the walls with hydrogen, and they were able to increase the D content of the plasma from D/(D+H)=0.3 to 0.5. However, less than 10% of the H inventory could be removed from the walls by this isotope-exchange mechanism while the retention of D from the ICWC plasma was almost three times higher. The fuel can also be removed by He-ICWC, and results again from JET indicate D being efficiently removed but almost 80% of the injected He being retained in the vessel. At Tore Supra, for its part, pulsed ICWC discharges (¡1 s) have been carried out and the retention could be decreased well below the amount of pumping without compromising the cleaning or isotope-exhange rate on the walls.

So far, however, the data on the applicability of ICWC in cleaning the vessel walls from fuel-containing layers during changeover from H or D to He plasmas is rather scarce. This deficiency was addressed at AUG during a dedicated He-ICWC experiment before the onset of the 2015 helium campaign. In the experiment [17], two ion cyclotron resonance heating (ICRH) antennas were used during 20 discharges at 2.0 T, having a total duration of 180 s. The RF power was 100−200 kW at 30 MHz and He was injected into the torus from the outer midplane such that the pressure was $1 - 5 \times 10^{-4}$ mbar. The fuel content of the vessel was monitored by (i) determining the evolution of the D and He content of the plasma before, during, and after ICWC discharges by measuring the CX flux of neutrals by neutral particle analysers (NPA), (ii) evaluating the temporal evolution of the D_α (656.1 nm) and He I (667.8 nm) spectral lines in the divertor and main-chamber regions, (iii) studying the composition of the exhaust gas using mass spectrometry, and (iv) measuring the D_2 and He contents of W samples exposed to plasmas in the outer midplane.

Significant release of D from the wall structures could be observed during ICWC. This we notice from the CX data for neutral D flux (see figure 1a), which show a peak in the beginning of the ICWC discharges and a gradual decrease towards the end of the experiment. Similar trend was observed by the spectroscopic measurements. The release

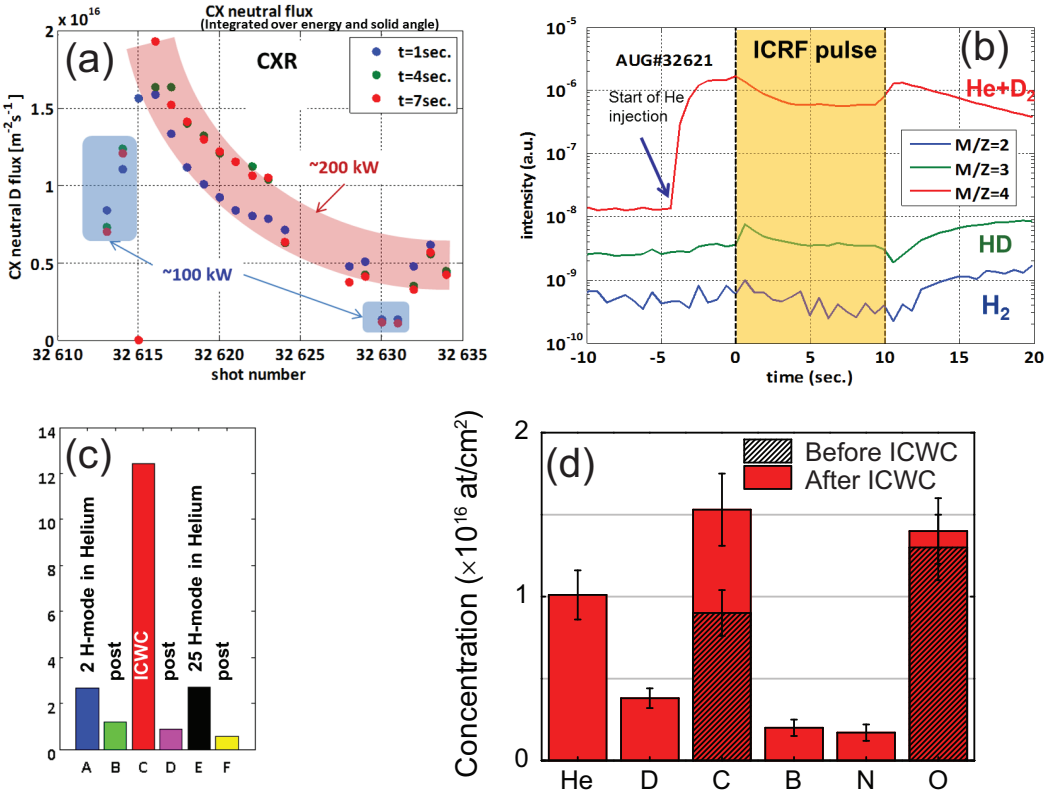

Figure 1. (a) Evolution of the CX neutral D flux during the ICWC experiment. (b) Time traces for selected M/Z signals before, during, and after an ICWC pulse. (c) Number of D_2 molecules removed during H-mode shots in helium (A and E), overnight outgassing (B, D, and F), and the actual ICWC experiment. The overall duration of the measurement period was 170 hours. (d) Surface densities for selected elements on W samples at the outer midplane before and after the ICWC experiment

rate was quantified on the basis of mass spectrometry. From the temporal behaviour of the partial pressures of H_2, HD, and D_2 (+He) signals during each discharge (figure 1b) the total amount of D being removed by ICWC integrates to 13 Pa m^3, including 15 min outgassing between discharges (phase C in figure 1c). During overnight outgassing (phases B, D, and F) the amount remained ¡1 Pa m^3 while during two H-mode plasma discharges in helium before ICWC (phase A) and during 25 H-mode discharges after ICWC (phase E) the D_2 release of 3 Pa m^3 was measured. Simultaneously, the He content of the plasma increased from He/(He+D+H)=0.4 (phase A) to 0.8 (phase E).

The efficiency of ICWC was also estimated by surface analyses of bulk W samples before and after their exposure to the ICWC discharges (figure 1d) [18]. The samples were studied using Elastic Recoil Detection Analysis (ERDA) with a 10-MeV $^{28}Si^{3+}$ beam for the detection of He and D and Time-of-Flight ERDA with a 36-MeV $^{127}I^{8+}$ beam to determine the concentrations of heavier impurities. As a result of ICWC, co-deposited layers containing D, B, C, N, and O were formed on all the samples, with concentrations in the range of $0.2 - 1.5 \times 10^{16}$ at cm^{-2}. Boron originates from

regular boronizations of the AUG vessel, nitrogen from seeding experiments carried out in AUG, while C is most likely released from PFCs with damaged W coatings on graphite substrates. It is worth noting that the initial C content of the W surfaces was relatively high, 10^{16} He cm^{-2}, thus the net amount of C deposited on the surfaces is similar or slightly larger than the surface density of D. The helium content of the co-deposits, for its part, is a factor of two larger than the amount of D measured in them, up to 10^{16} He cm^{-2} (see figure 1d). This suggests that He may substitute a substantial fraction of hydrogen atoms retaining on the samples during ICWC.

One should, however, keep in mind that the analysed samples reflect a situation only at a particular location of the vessel, here at the outer midplane. As discussed above, the data in figure 1 show that globally D is removed from PFCs but, besides being pumped away from the torus, the removed particles can migrate in the scrape-off layer (SOL) plasma and accumulate in shadowed areas of the torus through multiple erosion-deposition steps [19]. This is a potential scenario since the W samples were located barely in front of the shadow of limiter structures during the experiment.

3. Erosion, deposition, and surface modifications of W PFCs at AUG

3.1. Samples and their characterization

The interaction of W PFCs with helium was investigated by exposing four poloidal rows of different samples to ELMy H-mode discharges in He at the outer strike-point (OSP) region of the AUG divertor [20]. The samples were mounted on two target tiles - two rows per target tile and 6 samples in each row - made of bulk W which were transferred to the desired location using the upgraded divertor manipulator (DIM-II) of AUG [21], see figure 2a.

For each row, a different sample type was selected. On the first tile, bulk W samples were mounted at the centre, while W-coated (thickness 30 nm) graphite marker samples were positioned magnetically downstream of them. On the second target tile, the centre row consisted of W samples pre-modified by He exposure in the high heat-flux device GLADIS [22] (denoted by T1-T6) while in the edge row bulk Mo samples had been positioned. The marker samples were used to determine erosion of W during the actual plasma experiment, the purpose of the Mo samples was to estimate re-deposition of W, while the two sets of W samples provided information on the changes in the surface morphology as well as the formation or erosion of fuzz and retention of He on them.

The pre-modified samples contained a variety of nanostructures on the surfaces with a layer thickness of $2-3$ μm. The nanostructures were produced by mounting bulk W samples in GLADIS on a target plate and exposing them to a pure He beam with an energy of 37 keV. A photograph of the sample surface after irradiation is shown in figure 2b. At the centre of the holder, the surface temperature was 2300 K and the He fluence around 1.0×10^{24} He$^+$ m^{-2}, while at the edge the corresponding values were 1300 K and 0.4×10^{24} He$^+$ m^{-2}. The fluence and surface temperature clearly

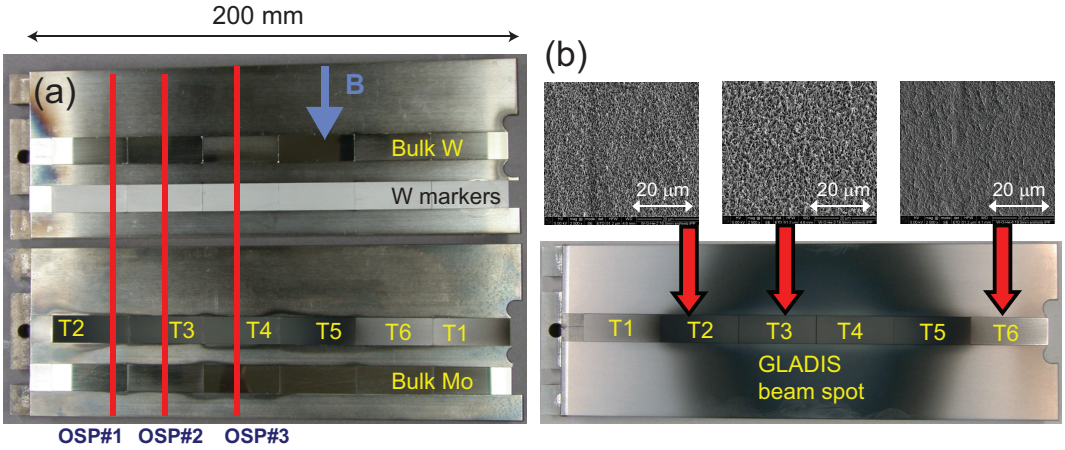

Figure 2. (a) Photograph of the 4 sample types mounted in the divertor target tiles after the plasma experiment. The pre-modified samples are labelled with symbols T1-T6 and the OSP positions for the three phases of the plasma experiment have been marked with red lines. Private flux region is located on the very left. (b) Photograph of the pre-modified probes T1-T6 after their exposure in GLADIS together with SEM images of the modified surfaces of T2, T3, and T6.

favoured nanostructure formation while the energy was much higher (keV) compared to the typical values in tokamak edge plasmas (eV). Nevertheless, based on microscopy analyses, also at these high energies tendril-like networks had been formed on practically all the samples. At the center (samples T2-T5), the nanoscale network largely resembled fully developed fuzz while in the peripheral zone the surface modifications were not that distinct. The thickness of the modified layer on samples T3 and T4 was approximately 2 μm and contained significant helium inventories from the GLADIS treatment.

The most extensively modified samples T2-T4 were mounted closest to the OSP positions during the experiment while the samples with more benign surface modifications towards the upper edge of the target tile. The surface morphology of all the samples was monitored by scanning electron microscopy (SEM) and focused ion beam (FIB) studies. The erosion of the marker coatings was determined by Rutherford Backscattering Spectroscopy (RBS), using 2.0-MeV $^4He^+$ ions for the samples before and after the plasma experiment. After that all the samples were measured by Nuclear Reaction Analysis (NRA), where 3.8-MeV $^3He^+$ ions were applied to determine the deposition of different elements, primarily D, B, C, and N on the surfaces. The helium content of the samples is discussed in section 4.

3.2. Plasma conditions during sample exposure

The W samples were exposed to plasma discharges in the lower single null (LSN) configuration on AUG with the following parameters: plasma current $I_p = 0.8$ MA, toroidal magnetic field $B_t = 2.5$ T, auxiliary heating with electron cyclotron resonance heating (ECRH) of 2.6 MW at 140 GHz, neutral beam injection (NBI) of 2.1 MW with

equal share of H and He beams, and ICRH of 4.0 MW at 36.5 MHz. The average core density was $n_e^{core} = 9 - 10 \times 10^{19}$ m^{-3} and electron temperature $T_e^{core} = 3.0$ keV during the 7-s long flat-top phase of an individual He discharge. Altogether 25 identical shots were carried out such that the OSP position was varied between three poloidal locations (marked in FIG. 2) [20]. The overall exposure times for the three phases were 100 s, 60 s, and 10 s, respectively. The D content of the plasma remained at a constant level of 10% during the experiment and slowly decreased to ¡5% by the end of the He campaign. The H and He contents showed large fluctuations due to H beams used for plasma heating and, on average, the He content did not increase much from the starting value of 80% after ICWC (see section 2). One should notice that the previous boronization of AUG with B_2D_6 took place only one week ahead of the experiment, thus a large amount of boron was still around on the vessel walls and could be mobilized by the SOL plasma to result in a large B influx in the divertor region [23].

In the first part of the experiment (100 s), the OSP was poloidally set on the lowermost samples such that the pre-modified sample T2 could be exposed. This way one could investigate whether the nanoscale features were grown during the exposure. In the second phase, the OSP was moved upwards such that the sample T3 with a coral-like surface was subjected to the highest particle and power fluxes. Now the idea was to investigate erosion of existing W nanostructures by ELMs as well as further modifications of the surfaces. In phase I, only type III ELMs in the kHz regime were produced while in phase II, type I ELMs at 120-Hz frequency were observed, resulting from reduced fuelling between the two phases. In the third phase, the OSP was further raised and small N_2 blips were applied to study the impact of N on the nanostructures; these results will not be discussed here.

Based on Langmuir probe measurements in the vicinity of the OSP, the ion saturation flux was some $2 - 2.5 \times 10^{23}$ m^{-2} s^{-1} and $T_e^{OSP} = 20 - 25$ eV. Assuming that the impinging ions are mostly He^+, we obtain for the impact energy $E_{in} = 100 - 150$ eV by making use of the formula $E_{in} = 3T_e + 2T_i$ [24] with the electron and ion temperatures (T_e and T_i, respectively) being approximately equal for He^+. This energy is well above the threshold of 20 eV for fuzz formation (see section 1). From the 80% He content of the plasma, the fluence during phases I and II of the experiment was $1 - 2 \times 10^{25}$ He^+ m^{-2}, an order of magnitude more than the 10^{24} He^+ m^{-2} limit mentioned in section 1. The surface temperature of the samples could not be directly measured but infrared measurements from neighbouring standard wall tiles indicate $T_s > 800$ K. The samples, however, were much hotter due to their poor thermal contact with the target tiles, thus values higher than 1000 K are expected. Thus, all the criteria for nanostructure growth and formation were fulfilled in phases I and II. On the other hand, in phase II the impact energy of helium ions during the ELMs is estimated to $E_{in,max}^{ELM} = 1.2 - 1.3$ keV by making use of the approximate formula $E_{in,max}^{ELM} \approx 4.23 T_e^{ped}$ [24] with $T_{e,max}^{ped} \sim 300 - 350$ eV, and this energy is sufficient to result in significant sputtering of the nanostructures. Thus, in phase II, a competition between nanostructure growth and destruction exists.

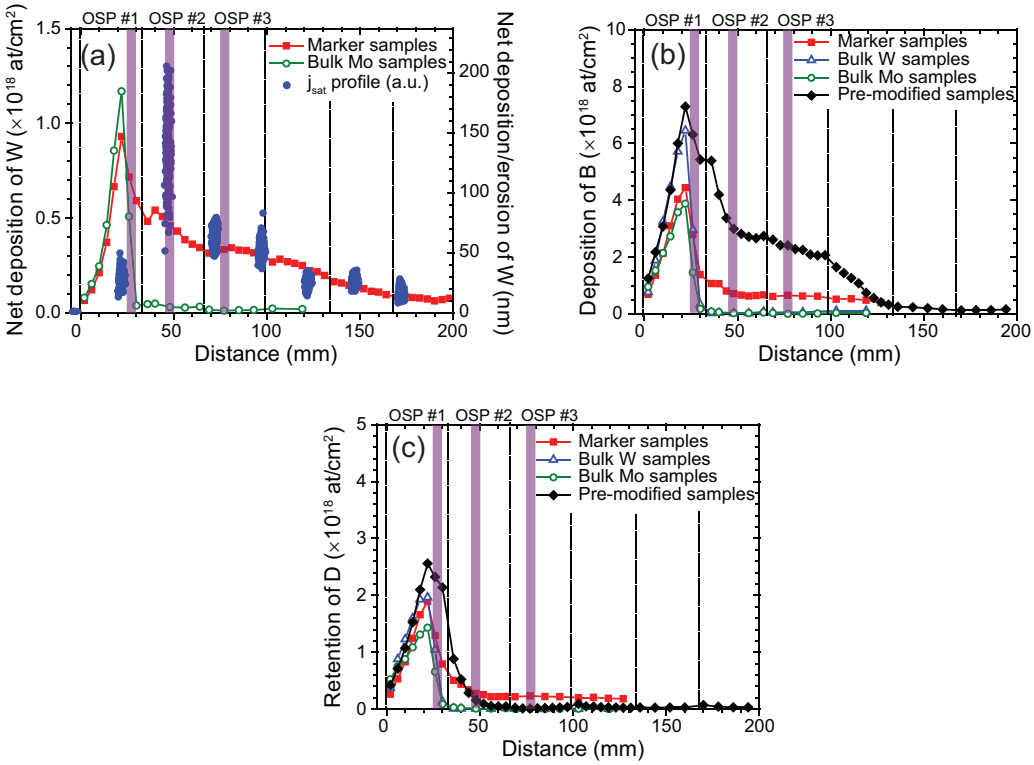

Figure 3. (a) Poloidal net deposition/erosion (positive/negative values) profile for the W marker sample and re-deposition profile for W on the bulk Mo samples. For comparison, the profile for the ion saturation flux during phase II of the experiment is shown. (b) Poloidal deposition profile for B and (c) for D on the different samples. The purple bars denote the OSP positions during the three phases of the experiment. Notice the different scales of the vertical axes.

3.3. Results and conclusions

The main observations can be summarized as follows:

- No noticeable net erosion has taken place, not even close to the actual OSPs, but the amount of W on the marker samples has increased by dozens of nm as a result of the plasma exposure (figure 3a). Thus, the entire OSP region is dominated by net deposition with the thickest layers in the private flux region (PFR), below all the OSPs of the experiment. This is in sharp contradiction with what has earlier been reported for D plasmas: a distinct net erosion peak at the strike point and net deposition regions surrounding it [25]. Figure 3, in contrast, suggests that in helium plasmas a strong influx of material is established from the main chamber to the divertor, where it is further transported along the magnetic field lines and poloidally by the $\mathbf{E} \times \mathbf{B}$ drift towards the PFR [26].
- All the samples are covered with thick co-deposited layers (up to 1 μm) consisting mainly of D, B, C, N, O, and W. The deposition profiles are qualitatively similar to the net deposition profiles for W in figure 3a, as shown in figures 3b and c for B

and D, respectively, but some clear differences can be observed as well. The B and W curves in figures 3b and c agree with the shape of the flux profile of He^+ ions as indicated in figure 3a for phase II discharges while the D profile shows only the peak in the PFR. This could indicate that B and W are travelling to the divertor region all the way from the main chamber while D is embedded in the deposits from more local sources in the divertor. New experiments and careful spectroscopic measurements in the main chamber and in the divertor region are needed to verify this hypothesis.

- The rougher the sample surface, the more material is deposited on it, particularly above the OSPs. The strongest deposition is measured on the pre-modified samples with a large effective surface area while on the smooth bulk W and Mo samples deposition outside the PFR is almost non-existent. This is in line with the conclusions made in [10, 27] on rough surfaces favouring accumulation of material in shadowed valleys behind protruding surface peaks. The smooth Mo and bulk W surfaces respond quite differently to the impinging particles such that they are efficiently re-eroded or reflected and no noticeable deposit can form.
- For tungsten, however, the deposition peak in the PFR is almost independent of the surface roughness but relatively rough marker samples and smooth bulk Mo samples indicate net deposition being comparable (figure 3a). This can be interpreted by noticing that below the strike point the cold plasma conditions favour layer-by-layer growth of material without re-erosion such that the memory of the original surface is lost after a couple of seconds. On the other hand, on the pre-modified and bulk W samples much more impurities in the PFR than on the two other samples have been measured but this could be simply due to their different toroidal positions, as one can notice in figure 2.
- No signs of nanostructure growth or erosion are observed on the pre-modified samples, nor on the bulk W samples. This is attributed to the deposited layer being quickly formed on the surface and covering all the nanoscale features, thus protecting them from further exposure as FIB images in figure 4 illustrate. Around the OSP, the top part of a few individual corals appears to have been cut off (see purple and yellow zoom-ins in figure 4a), possibly because they have formed leading edges and ELMs have then eroded them. Deeper in the PFR the co-deposit can be seen to consist of ¿20 sublayers (figure 4b).

We conclude that erosion of W surfaces and nanostructure formation or growth is overcompensated by local deposition of material in between ELMs, possibly resulting from erosion in the main chamber. The situation is quite unlike the case during D operations when large net erosion is typically measured around the strike point [25]. Different main-chamber sources are indeed plausible explanations to the apparent discrepancies: in our experiment, ICRH-heated plasmas were applied leading to enhanced sputtering of W directly by singly or doubly ionized He ions on the limiter structures surrounding the ICRH antennas and, additionally, by ELMs [28].

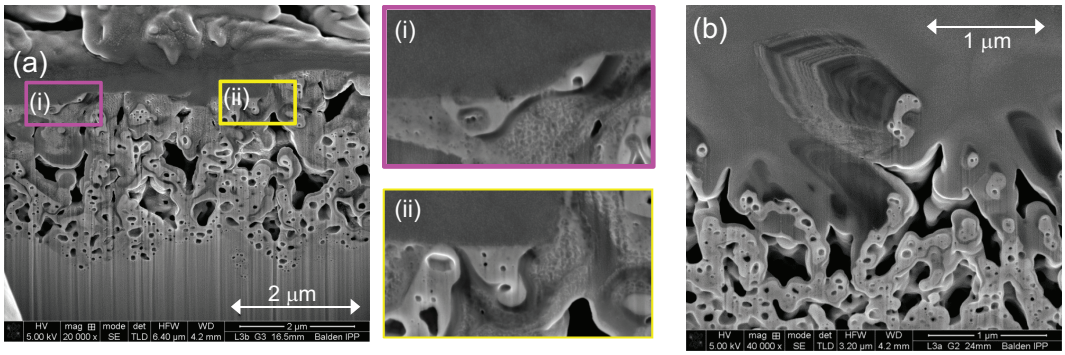

Figure 4. (a) FIB images of the sample T3 close to the OSP. The two zoom-ins (i) and (ii) of the interface between the original nanostructure and the deposited layer have been marked with purple and yellow rectangles. (b) FIB image of the sample T2 in the PFR with the layered structure of the co-deposit.

The qualitatively different deposition patterns on the four sample types are also affected by the balance between erosion and deposition phenomena. On the smooth bulk W samples, the two processes are equally important while in the case of rougher samples, re-erosion is further reduced and net deposition takes over.

4. Retention of helium in tungsten samples

The He content of selected samples was measured using foil-ERDA with 15-MeV $^{16}O^{5+}$ ions and time-of-flight ERDA with 23-MeV $^{127}I^{6+}$ ions. In both cases, only the topmost surface layer (some 50-100 nm) could be analysed, but based on earlier studies, under low-energy and low-flux irradiations, as is the case in the AUG experiment, He is typically retained close to the surface due to its high probability of being trapped in defects [29]. As discussed in section 1, this will lead to the formation of a diffusion barrier in this implantation zone, which tends to limit subsequent retention of H and D in the material [7]. However, the actual accumulation of helium in W depends strongly on the exposure conditions and the surface morphology: the higher the surface temperature and the applied helium flux as well as the more porous the sample becomes due to fuzz growth, the more He is retained in the material (up to 7 at.%) with the depth profile extending deeper than in W samples with a smooth surface [30]. All this influences the subsequent D and H retention as well.

The different ERDA profiles are shown in figure 5a for the analysed samples, located in the vicinity of the OSP, on the SOL side of it. On the bulk W samples, the He content is $1-3\times10^{16}$ He cm^{-2}, which is of the same order of magnitude as the surface densities measured on the W samples after the ICWC experiment (see section 2). The profile is also relatively flat with some point-to-point oscillations but no major increase in retention towards the PFR, as was, e.g., the case for D (see figure 5b where the data of figure 3c is reproduced at a higher magnification). This indicates that He indeed stays in the vicinity of the surface, either trapped in defects and pores or the topmost layer

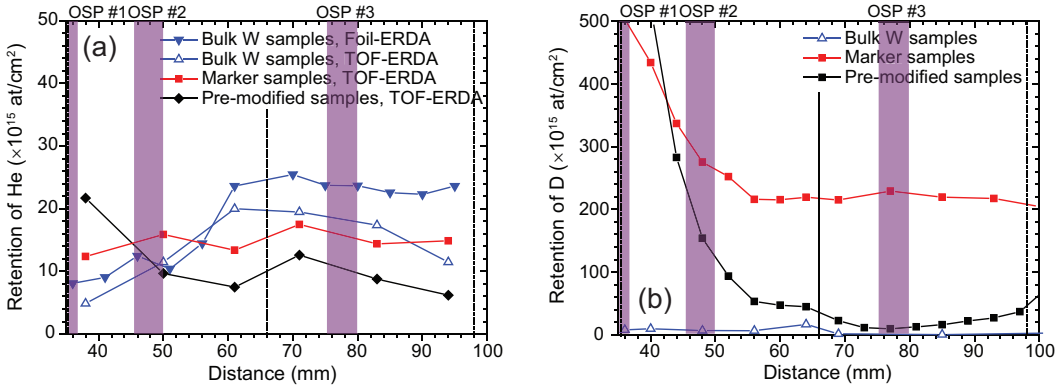

Figure 5. (a) Poloidal retention profile for He on the different samples around the OSP region. (b) Poloidal retention profile for D on the different samples around the OSP region (zoom in of the data in figure 3c). The purple bars denote the OSP positions during the three phases of the experiment.

of the growing co-deposit, as proposed in [29, 31]. Our results also support the idea of saturation such that the surface densities would remain $< 10^{17}$ He cm^{-2} [32].

For the pre-modified and coated marker samples, ERDA indicates the He content to be comparable to that of bulk W samples or slightly lower. However, Thermal Desorption Spectroscopy (TDS) data up to 1000°C suggest the total He inventory to be $3-4$ times higher on these samples (figure 6) than on bulk W, meaning that whenever the surface turns rough or porous, the penetration depth increases drastically. Interestingly, both ERDA and TDS indicate that equally much He is accumulated on both pre-modified and coated samples but all the results have to be treated with caution since on one hand the original nanostructured surface contained He from the GLADIS exposure and, on the other hand, a significant fraction of helium on the samples may have desorbed during the time between their exposure and analyses (up to 10 months, including cutting samples into smaller pieces). From the TDS curves one also notices the qualitatively different release behaviour of helium. On bulk W, the two release peaks at $\sim$ 700°C and $\sim$ 900°C are comparable while for the marker samples the majority of the helium is released only at $\sim$ 1000°C. The pre-modified sample behaves similarly but the release at higher temperatures takes even longer, meaning either release from tightly-bound traps or deep from the sample.

5. Conclusions

In this article we have studied plasma-wall interaction effects in the full-W ASDEX Upgrade during its dedicated helium campaign in 2015. Relatively clean plasmas with a He content of ¿80% could be obtained by applying ICWC discharges upon changeover from D to He. The D content of the plasma then slowly decreased during the entire He campaign while the He concentration did not change much due to frequent heating of the plasmas with hydrogen NBIs. Surface analyses of W samples, however, indicated co-

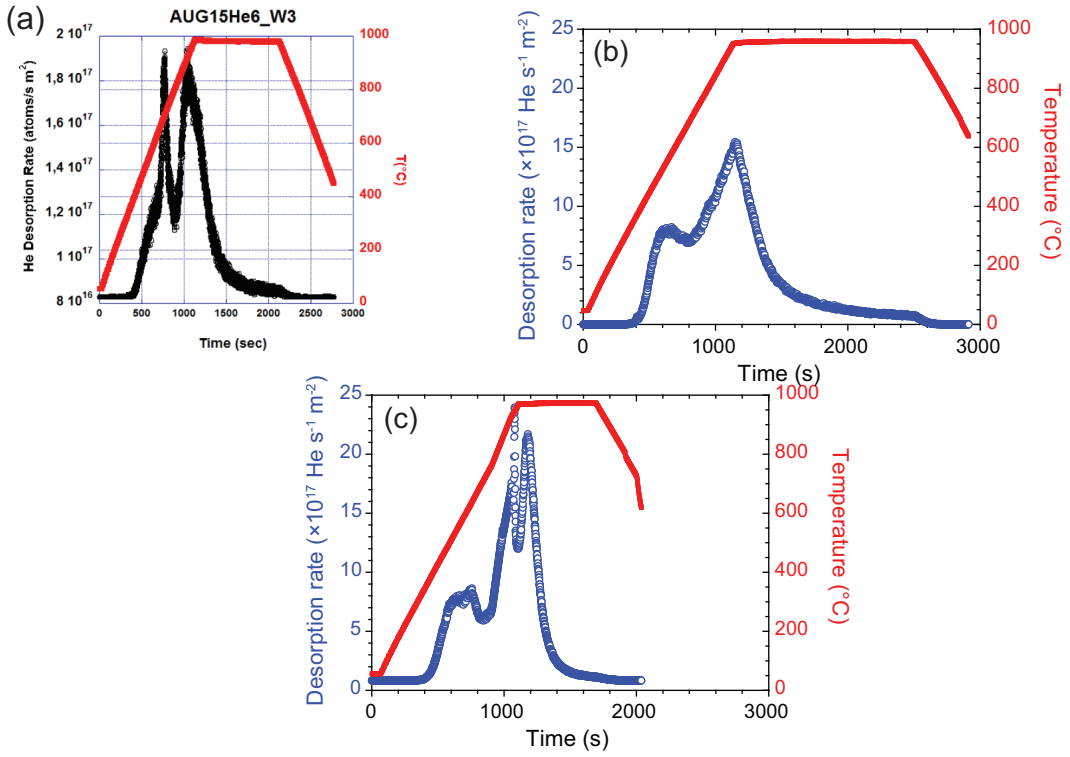

Figure 6. TDS data for the release of helium from (a) a bulk-W sample, (b) a marker sample, and (c) the pre-modified sample T4, all extracted close to OSP#3. The total release of helium in all the cases is: (a) 5.7×10^{-3} mbar l, (b) 20.9×10^{-3} mbar l, and (c) 19.7×10^{-3} mbar l.

deposited layers being formed on them which contained, besides He, significant amounts of D. This can be explained by multiple erosion-deposition steps albeit globally D was released from the PFCs.

When exposing different W samples to ELMy H-mode helium plasmas in the outer strike-point region of the divertor, no net erosion was observed but the sample surfaces had been covered with co-deposited layers. The layers were the thickest in the private flux region and extended throughout the OSP region in the case of rough and modified surfaces. Also, no clear signs of nanostructure growth or destruction could be seen. Since under D plasma operations the OSP co-incides with a region of prominent net erosion, we conclude that in He plasmas extra W sources, presumably in the main chamber, result in efficient coverage of the W surfaces during the first couple of seconds. The growth of such layers may impact the operation of future fusion reactors. Dedicated lab experiments and modelling efforts in the presence of impurity mixes are needed to elucidate the issue further and determine its significance for the operation of ITER: If the wall source during He plasmas is much higher than in comparable D discharges, it will be challenging to extrapolate the results obtained during the He phase to the latter operational phases. In fact, the deposition pattern for boron observed on AUG can be considered a proxy for beryllium in the ITER divertor. In helium plasmas, the erosion

of beryllium is expected to be at least twice as strong as during D or D-T operations, meaning that thick co-deposits and increased fuel retention would be expected.

Acknowledgements

This work has been carried out within the framework of the EUROfusion Consortium and has received funding from the Euratom research and training programme 2014-2018 under grant agreement No 633053. The views and opinions expressed herein do not necessarily reflect those of the European Commission or the ITER Organization.

References

[1] Philipps V 2011 *Journal of Nuclear Materials* **415** S2
[2] Brezinsek S *et al* 2015 *Journal of Nuclear Materials* **463** 11
[3] Neu R *et al* 2013 *Journal of Nuclear Materials* **438** S34
[4] Douai D *et al* 2015 *Journal of Nuclear Materials* **463** 150
[5] Baldwin M *et al* 2008 *Nuclear Fusion* **48** 035001
[6] Petty T J *et al* 2015 *Nuclear Fusion* **55** 093033
[7] Ueda Y *et al* 2009 *Journal of Nuclear Materials* **386-388** 725
[8] Alimov V Kh *et al* 2009 *Physica Scripta* **T138** 014048
[9] Baldwin M *et al* 2011 *Nuclear Fusion* **51** 103021
[10] Hakola A *et al* 2014 *Physica Scripta* **T159** 014027
[11] Kajita S *et al* 2009 *Nuclear Fusion* **49** 095005
[12] Kajita S *et al* 2011 *Journal of Nuclear Materials* **418** 152
[13] Ueda Y *et al* 2011 *Journal of Nuclear Materials* **415** S92
[14] Wright G M *et al* 2012 *Nuclear Fusion* **52** 042003
[15] Doerner R P *et al* 2016 *Physica Scripta* **T167** 014054
[16] Douai D *et al* 2011 *Journal of Nuclear Materials* **415** S1021
[17] Douai D *et al* 2016 Changeover from Deuterium to Helium with Ion Cyclotron Wall Conditioning and diverted plasmas in ASDEX Upgrade *Proc. 22nd Int. Conf. on Plasma Surface Interactions in Controlled Fusion Devices* (Rome, Italy) p P3.116
[18] Petersson P *et al* 2016 Investigation of probe surfaces after ion cyclotron wall conditioning in ASDEX Upgrade *Proc. 22nd Int. Conf. on Plasma Surface Interactions in Controlled Fusion Devices* (Rome, Italy) p P3.118
[19] Strachan J D *et al* 2008 *Nucl. Fusion* **48** 105002
[20] Brezinsek S *et al* 2016 Erosion of He pre-exposed tungsten samples by He plasmas in the divertor manipulator of ASDEX Upgrade *Proc. 22nd Int. Conf. on Plasma Surface Interactions in Controlled Fusion Devices* (Rome, Italy) p P1.68
[21] Herrmann A *et al* 2015 *Fusion Engineering and Design* **98-99** 1496
[22] Greuner H *et al* 2011 *Journal of Nuclear Materials* **417** 495
[23] Rohde V *et al* 2007 *Journal of Nuclear Materials* **363-365** 1369
[24] Guillemaut C *et al* 2015 *Plasma Physics and Controlled Fusion* **57** 085006
[25] Hakola A *et al* 2016 *Physica Scripta* **T167** 014026
[26] Hakola A *et al* 2016 ERO and PIC simulations of gross and net erosion of tungsten in the outer strike-point region of ASDEX Upgrade *Proc. 22nd Int. Conf. on Plasma Surface Interactions in Controlled Fusion Devices* (Rome, Italy) p P1.59; *Nuclear Materials and Energy* (in press)
[27] Schmid K *et al* 2015 *Journal of Nuclear Materials* **463** 66
[28] Bobkov V *et al* 2017 *Plasma Physics and Controlled Fusion* **59** 014022
[29] Tokunaga K *et al* 2003 *Journal of Nuclear Materials* **313-316** 92

[30] Woller K B *et al* 2015 *Journal of Nuclear Materials* **463** 289
[31] Hu C *et al* 2016 *Fusion Engineering and Design* **112** 117
[32] Hino T *et al* 1999 *Journal of Nuclear Materials* **266-269** 538